Excess photon ionization and harmonic generation through an autoionizing resonance

Jian Zhang and S. J. van Enk
Max-Planck Institut für Quantenoptik, Hans-Kopfermann-Strasse 1, D-85748 Garching, Germany
(Received 13 February 1995; revised manuscript received 9 August 1995)

We analyze above-threshold ionization through an autoionizing resonance and show that this process is strongly enhanced when the photon is tuned near the minimum of the primary photoionization peak; the enhancement occurs also when the free-free transitions are taken into account. We demonstrate that this property can be exploited to enhance the harmonic generation.

PACS number(s): 32.80.Dz, 32.80.Fb, 42.50.Gy

I. INTRODUCTION

It is well known that destructive quantum interferences lead to a minimum in the photon absorption [1] near an autoionizing (AI) resonance. Much theoretical and experimental work in laser spectroscopy has been centered around this subject in the last three decades. One type of application aims at generating short-wavelength radiation, either by amplification or by harmonic generation. In particular, the harmonic generation through a three-photon resonant AI state has been explored [2,3]. Recently, for instance, it has been shown that third-harmonic generation is enhanced appreciably through the combination of population trapping in the AI state and electromagnetically induced transparency for the generated harmonic radiation [4].

Another example of applications is to resonantly enhance the excitation to an AI resonance through the absorption minimum of another intermediate AI state [5]. Closely related to this is the recent experimental investigation of excess-photon detachment through AI resonances of alkaline negative ions [6,7]. In this work we present a theoretical analysis of a similar process, the above-threshold ionization (ATI) through an autoionizing resonance, and we show analytically that the destructive interference giving rise to the absorption minimum at the AI state leads to a *maximum* in the next ionization step. Thus, the ATI process is enhanced, not only because of the presence of the intermediate resonance, but also because of the presence of the minimum. The second ionization peak has its maximum when the photon is tuned *not* on resonance with the AI state, but at the absorption minimum.

Here we combine these two ideas and show by explicit calculations that these processes are eminently suitable to enhance the third-harmonic generation in a system that is two-photon resonant with an AI state: the fact that the minimum of the two-photon ionization probability coincides with the maximum of the three-photon coupling amplitude optimizes the third-harmonic generation, while the loss due to ionization is kept at a minimum.

The main reason to study two-photon resonant third-harmonic generation through an AI resonance is to search for more efficient ways of producing short-wavelength radiation. Of course, third-harmonic generation in neutral atoms through intermediate *bound* states is a well-known efficient method [8], but the wavelength is necessarily restricted to be in the optical range (except in strongly bound atoms like He). This restriction can be lifted by using doubly excited states in two-electron systems, which may be above the ionization threshold, as intermediate resonances. As mentioned above, third-harmonic generation through a *three-photon* resonant AI state has been investigated, but using *two-photon* resonant AI states in principle allows one to go even higher in energy. Since the AI state not only resonantly enhances the third-order nonlinear susceptibility, but also reduces the ionization at the two-photon level, this scheme has definite advantages over third-harmonic generation through pure continuum states.

This analysis is also related to the interest in understanding the role of the electron-electron correlations in ATI spectra of two-valence electron atoms under intense laser fields, and to the question of double ionization (for recent experiments and discussions see, e.g., Refs. [9–11]). Compared to previous theoretical work on excess photon ionization of AI states [12], we include the continuum-continuum (C-C) coupling, and show that this inclusion leads to modifications of the photoelectron spectrum and of the ionization profile.

II. THEORY

We consider an atomic system whose level scheme is shown in Fig. 1. In order to describe this system, we employ the resolvent operator formalism, which has been applied before to single [13] and multiphoton [14] autoionization (see also [15] where the radiative coupling between two manifolds of AI states in Sr is discussed). Details of the derivation will be given in the Appendix. Here we will only discuss the main assumptions and ingredients, and we give analytical results for several quantities of interest.

A. Basic assumptions

There are basically two assumptions we make. First, we assume a Fano-type parametrization for the coupling to the AI resonance and its associated continuum. This is correct as long as there is only a single AI state in resonance with the light field. Apart from this, we do not make any assumption about the form of the C-C coupling. Second, we treat the C-C coupling in a perturbative way: we do not consider multiple transitions between the two continua. This assumption is correct for sufficiently low intensity, a condition which will be specified below. At higher intensities, when these multiple transitions would be important, other continua, both

 © 1995 The American Physical Society

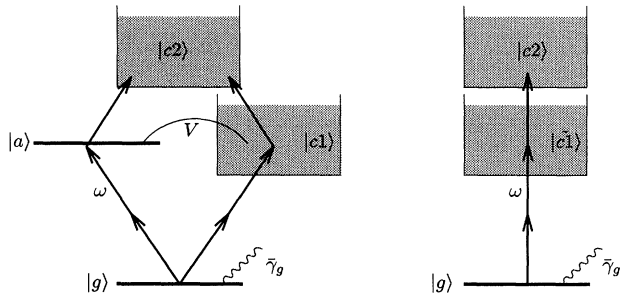

FIG. 1. Energy level scheme of the model system. Left: in terms of a doubly excited state $|a\rangle$ coupled by the configuration interaction V to the pure continuum $|c_1\rangle$. Right: equivalent model, in terms of a structured continuum $|\tilde{c}_1\rangle$.

higher-lying ones and the ones with different angular momenta, would enter the problem, so that the model we use would be invalid anyway. For the parameters we choose in this paper, and for a photon energy of about 5 eV, this implies a C-C saturation intensity of $I\approx 10^{14}$ W/cm^2 (cf. also [16]), and we remain well below this intensity. For larger photons the saturation intensity increases in general. We now take a closer look at the atomic system of Fig. 1.

The ground state $|g\rangle$ is coupled via an M-photon process to the vicinity of an isolated autoionizing resonance $|a\rangle$, which decays to a continuum $|c1\rangle$ by autoionization. Both $|a\rangle$ and $|c1\rangle$ are coupled to a higher-lying continuum $|c2\rangle$ by a one-photon dipole transition. This coupling may represent both pure free-free transitions (in which the outer electron makes a transition) and a far off-resonant core transition (in which only the inner electron is involved). The states $|a\rangle$ and $|c1\rangle$ are coupled by the configuration interaction V, and can be diagonalized to form a structured continuum $|\tilde{c}1\rangle$ [1].

The M-photon dipole moment $\mu^{(M)}_{g\tilde{c}1}$ coupling the ground state to the continuum $|\tilde{c}1\rangle$ can be parametrized as

$$\mu^{(M)}_{g\tilde{c}1}=\mu^{(M)}_{gc1}\frac{\epsilon_{c1}+q}{\epsilon_{c1}-i}, \tag{1}$$

and $\mu^{(M)}_{\tilde{c}1g}=(\mu^{(M)}_{g\tilde{c}1})^*$. Here $\epsilon_{c1}\equiv(E_{\tilde{c}1}-E_a)/\gamma_a$ is the energy of $|\tilde{c}1\rangle$ relative to the AI state, normalized by half the AI width $\gamma_a=\pi|V_{ac1}|^2$, and q is the M-photon asymmetry parameter, defined as (with $\mathscr{P}$ denoting the principal part)

$$q=\frac{\mu^{(M)}_{ga}+\mathscr{P}\int\mu^{(M)}_{gc1}V_{c1a}/(E_g+M\hbar\omega-E_{c1})dE_{c1}}{\pi\mu^{(M)}_{gc1}V_{c1a}}, \tag{2}$$

where V_{c1a} represents the Coulomb interaction between $|a\rangle$ and $|c1\rangle$. With this form of the coupling to the structured continuum $|\tilde{c}1\rangle$, $|\mu^{(M)}_{g\tilde{c}1}|^2$ has the familiar Fano profile [1]. The only assumption needed later is that the variation of the quantities q and $\mu^{(M)}_{gc1}$ with E_{c1} is negligible over the width of the AI state, which is correct if there is no other AI resonance present around the energy $E_g+M\hbar\omega$.

Making the same assumption for the one-photon coupling to the higher-lying continuum implies that the coupling between $|\tilde{c}1\rangle$ and $|c2\rangle$ has the same form as that between $|g\rangle$ and $|\tilde{c}1\rangle$,

$$\mu_{c2\tilde{c}1}=\mu_{c2c1}\left(\frac{q_{c2c1}+\epsilon_{c1}}{\epsilon_{c1}-i}\right), \tag{3}$$

which depends explicitly only on ϵ_{c1}, and where μ_{c2c1} and q_{c2c1} are intensity-independent atomic parameters, with q_{c2c1} defined analogously to (2),

$$q_{c2c1}=\frac{\mu_{c2a}+\mathscr{P}\int\mu_{c2c1}V_{c1a}/(E_{c2}-\omega-E_{c1})dE_{c1}}{\pi\mu_{c2c1}V_{c1a}}. \tag{4}$$

Again, q_{c2c1} and μ_{c2c1} may depend on both energies E_{c2} and E_{c1}, but this dependence is assumed slow on the scale of the resonance structure around the AI state. In integrals we encounter below, we can then take the values of these quantities at the resonant energies $E_{c1}=E_g+M\hbar\omega$ and $E_{c2}=E_g+(M+1)\hbar\omega$. The contribution of far off-resonant core transitions is to modify the asymmetry parameter through the principal part term in (4).

In most cases, the first term in the numerator of (4) dominates the second, and q_{c2c1} will be large even when q is small. We can then approximate the photoionization rate $\bar{\gamma}_a$ of the AI resonance $|a\rangle$ to the continuum $|c2\rangle$ by

$$\bar{\gamma}_a=\pi|\mu_{c2a}|^2\mathscr{E}^2\approx q^2_{c2c1}\pi^2|\mu_{c2c1}|^2\mathscr{E}^2\gamma_a, \tag{5}$$

with $\mathscr{E}$ the slowly varying electric field amplitude in a.u. A perturbative treatment of the C-C coupling is valid for intensities such that $\bar{\gamma}_a\ll\gamma_a$.

Finally, we introduce an additional decay width $\bar{\gamma}_g$ of the ground state due to the radiative coupling to other continua with different angular momenta, which is always present when $M>1$. This consideration not only makes the model more realistic, but also avoids some complications due to the vanishing width of $|g\rangle$ at the M-photon absorption minimum to $|\tilde{c}1\rangle$.

B. Analytical results

Here we give the analytical final results obtained by keeping the C-C interaction up to first order. In the numerical calculations of the next section, we included the next higher-order corrections. The derivations can be found in the Appendix.

We are interested in three quantities. We give expressions first for the photoelectron spectrum, second for the total population in the two continua, and third for the third-order nonlinear susceptibility $\chi^{(3)}$, which gives a measure for the third-harmonic generation in the special case where $M=2$.

These quantities can all be expressed in the matrix elements defined above, and in terms of the roots $x_\pm$ of the quadratic equation (A5) determining the time evolution of the atomic system. The photoelectron energy spectrum is calculated from the amplitudes $U_{\tilde{c}1}(t)$ and $U_{c2}(t)$ for the respective continua, as $|U_{\tilde{c}1}(t\to\infty)|^2+|U_{c2}(t\to\infty)|^2$. These quantities follow from (A6) and (A7) and are given by

$$|U_{\tilde{c}1}(t\to\infty)|^2=\frac{\gamma_g}{\pi\gamma_a^2}\left|\frac{\epsilon_{c1}+q}{(\epsilon_{c1}-x_+)(\epsilon_{c1}-x_-)}\right|^2, \tag{6a}$$

$$|U_{c2}(t\to\infty)|^2=\frac{\gamma_g\bar{\gamma}_a}{\pi q_{c2c1}^2\gamma_a^3}\left|\frac{qq_{c2c1}-i(\epsilon_{c2}+q+q_{c2c1})}{(\epsilon_{c2}-x_+)(\epsilon_{c2}-x_-)}\right|^2. \tag{6b}$$

The populations in the two continua for $t\to\infty$ are calculated by integrating these expressions over the whole spectrum. Using complex contour integration we obtain

$$P_{c1}=\int|U_{\tilde{c}1g}(t\to\infty)|^2dE_{c1}=\frac{\gamma_g}{\gamma_a}\left[\frac{(x_++q)^2}{(x_+-x_-)(x_+-x_+^*)\mathrm{Im}x_+}+\frac{(x_-+q)^2}{(x_+-x_-)(x_+^*-x_-)\mathrm{Im}x_-}\right], \tag{7a}$$

$$P_{c2}=\int|U_{c2g}(t\to\infty)|^2dE_{c2}=\frac{\gamma_g}{\gamma_a}\frac{\bar{\gamma}_a}{\gamma_a}\frac{1}{q_{\tilde{c}2c1}^2}\left[\frac{(qq_{c1c2})^2+(x_++q+q_{c1c2})^2}{(x_+-x_-)(x_+-x_+^*)\mathrm{Im}x_+}+\frac{(qq_{c1c2})^2+(x_-+q+q_{c1c2})^2}{(x_+-x_-)(x_+^*-x_-)\mathrm{Im}x_-}\right]. \tag{7b}$$

In the next section we will illustrate these results, and show that their consequences can be exploited to enhance harmonic generation.

Finally then, in the case where $M=2$, if we assume that $|c2\rangle$ has a dipole-allowed transition to the ground state, we can calculate the third-order nonlinear susceptibility $\chi^{(3)}$, as (with ϵ the normalized photon detuning)

$$\chi^{(3)}=\int\int\frac{\mu_{g\tilde{c}1}^{(2)}\mu_{\tilde{c}1c2}\mu_{c2g}}{(\epsilon-\epsilon_{c1})(\epsilon-\epsilon_{c2})}d\epsilon_{c1}d\epsilon_{c2}=\pi^2\left[i\frac{q+q_{c2c1}-\epsilon(qq_{c2c1}-1)}{\epsilon^2+1}-\frac{\epsilon^2+qq_{c2c1}+\epsilon(q+q_{c2c1})}{\epsilon^2+1}\right], \tag{8}$$

so that at low intensities ($\gamma_g\ll\gamma_a$) the third harmonic production is proportional to

$$|\chi^{(3)}|^2\propto\frac{[(1-qq_{c2c1})\epsilon+q+q_{c2c1}]^2+[\epsilon^2+(q+q_{c2c1})\epsilon+qq_{c2c1}]^2}{(1+\epsilon^2)^2}. \tag{9}$$

We will compare this result with the one obtained from a time-dependent calculation of harmonic generation, including ionization, in Sec. III.

III. NUMERICAL RESULTS AND DISCUSSIONS

To be specific, in all the following calculations we take $M=2$. The reason for this choice is twofold. First it relates to recent experiments on excess-photon detachment of Rb^-[7], and second it enables us to apply the theory to the study of two-photon resonant third-harmonic generation. This choice $M=2$ mainly determines the intensity dependence of the various decay rates and couplings in the system. We choose the atomic parameters as follows: we take $q=1$ (the q value of the autoionizing resonance in the experiment [7] is small), and $q_{c2c1}=10$, this quantity being large in general. We choose $\gamma_g=\gamma_a$ at a typical laser intensity $I=10^{11}$ W/cm^2, so that $\mu_{gc1}^{(2)}=7.9\times10^5\sqrt{\gamma_a}$ in atomic units. For $\bar{\gamma}_g$ we assume the same intensity dependence as for γ_g (i.e., $\bar{\gamma}_g$ describes two-photon ionization), and we choose $\bar{\gamma}_g=0.1\gamma_g$.

The C-C coupling strength is determined by $\mu_{c2c1}=1$ (a.u.), being a typical value for photon energies of about 5 eV [18]. For smaller photons μ_{c2c1} tends to be larger. For our perturbative approach to be valid, we need to satisfy $\pi\mu_{c2c1}\mathcal{E}q_{c2c1}\ll1$, which means $\bar{\gamma}_a\ll\gamma_a$. This implies that $I\ll0.0041$ (a.u.), i.e., $I\ll1.4\times10^{14}$ W/cm^2 (cf. [16]).

Figures 2(a) and 2(b) show the photoelectron energy spectra as defined in (6b) for two different laser intensities. In each plot, spectra for three different laser detunings are shown. Dramatic changes in the relative heights of the two ionization peaks occur when the photon is detuned near the two-photon ionization minimum. The position of this absorption minimum in nonzero field is by now a well-known fact seen also in many related works, and is determined by the minimum of the imaginary part of the root, say x_-, that has the smaller imaginary part (see [12]). The condition for the detuning is

$$\epsilon=-q\frac{\gamma_a+\bar{\gamma}_a-(\gamma_g+\bar{\gamma}_g)}{\gamma_a}. \tag{10}$$

For instance, it is this condition that, in the absence of incoherent decay, such as that represented by a nonzero $\bar{\gamma}_g$ and $\bar{\gamma}_a$, leads to population trapping [19] and to transparency [4].

This effect is more clearly seen when we plot the ionization rates to the two continua $|c1\rangle$ and $|c2\rangle$. Figure 3 shows the two continua populations in the long-time limit versus the photon detuning. The upper curves display the population of $|\tilde{c}1\rangle$ and the lower ones the population of $|c2\rangle$. Each pair of curves corresponds to a different laser intensity. From the left to the right curve the intensities are $I=3.16\times10^{10}$, 1.0×10^{11}, and 1.41×10^{11} W/cm^2, corresponding to $\gamma_g=0.1\gamma_a$, $\gamma_g=\gamma_a$, and $\gamma_g=2\gamma_a$, respectively. We can see a close correlation between the enhancement of the ionization to the second continuum and the minimum of the first ionization peak. We can obtain analytical understanding of this phenomenon from Eqs. (7a) and (7b): When Im x_- has a minimum, the ionization rate of the ground state has a minimum. Thus, the population in the first continuum $|c1\rangle$ must have a minimum as well. Indeed, the value of x_- ap-

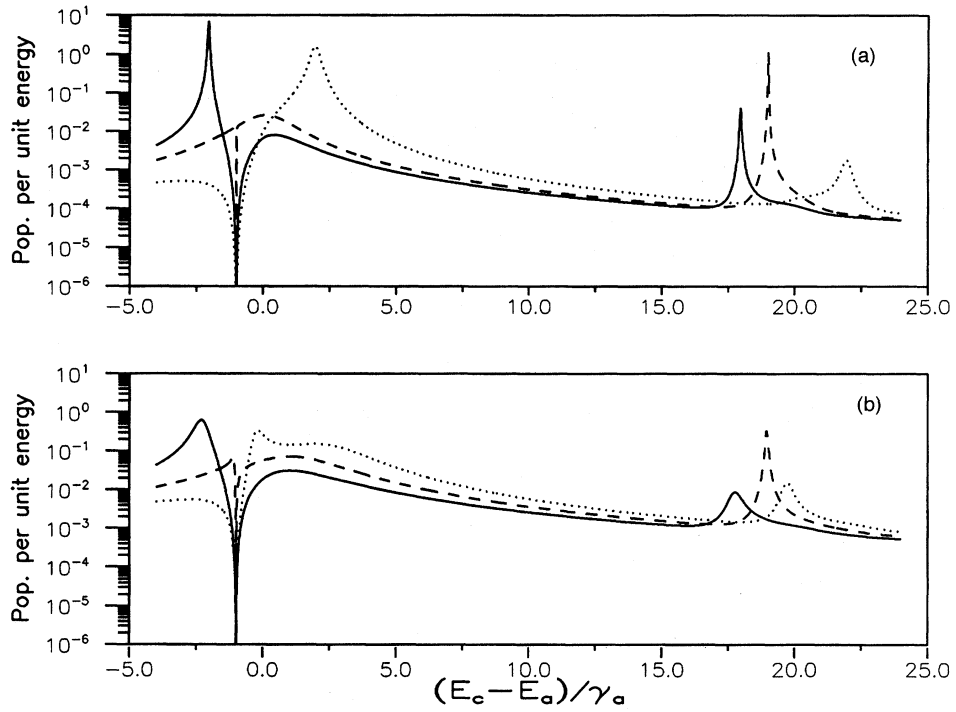

FIG. 2. Photoelectron energy spectra at (a) $I=3.16\times10^{10}$ W/cm^2 and (b) $I=1\times10^{11}$ W/cm^2 for a photon energy $\omega=20\gamma_a$. In (a) the photon detunings for solid, dashed, and dotted curves are $\epsilon=-2.0$, $\epsilon=-0.9$, and $\epsilon=2.0$, respectively. In (b) the photon detunings for solid, dashed, and dotted curves are $\epsilon=-2.0$, $\epsilon=-0.1$, and $\epsilon=2.0$. In both cases the detuning of the dashed curve is close to the absorption minimum (10).

proaches $-q$ near the minimum, and the zero in the denominator of (7a) is counteracted by a double zero in the numerator, so that P_{c1} will have a minimum. On the other hand, there is no such compensation in the expression (7b) for P_{c2}, so that the second continuum population will be maximum.

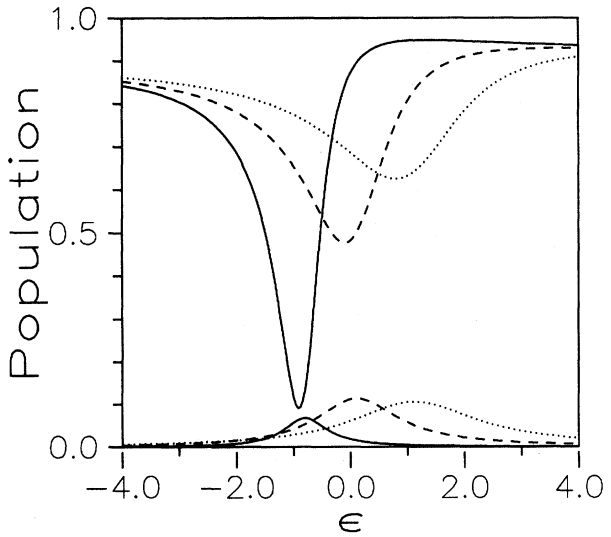

FIG. 3. Populations of continua $|\tilde{c}1\rangle$ and $|c2\rangle$ (scaled up by a factor of 2) as a function of detuning at three different intensities. Pairs of solid curves are calculated at laser intensities $I=3.16\times10^{10}$ W/cm^2, dashed curves are at $I=1.0\times10^{11}$ W/cm^2, and dotted curves are at $I=1.41\times10^{11}$ W/cm^2. The upper curves are the population of $|\tilde{c}1\rangle$ and the lower ones are the population of $|c2\rangle$.

In fact, from Fig. 3 we see that, for positive q, the maximum of the second ionization peak is slightly shifted to positive detuning compared to the minimum of the first peak, and this shift is larger for higher intensity. For negative q, irrespective of q_{c2c1}, we find that the shift is negative. Finally, we note that in previous work the C-C coupling was neglected, so that the second ionization peak is symmetric. In our case, however, we have due to the C-C coupling a finite q_{c2c1}, which leads to an asymmetric profile, which is, as usual, more pronounced the closer $|q_{c2c1}|$ is to unity.

An important conclusion, in agreement with experimental findings [6,7], is that the previous results indicate that the $(M+1)$-photon process in this system can be greatly enhanced at certain photon frequencies, while the M-photon process itself is suppressed. Therefore, we expect that the $(M+1)$st-order nonlinear process can be enhanced without an early saturation caused by the loss of the ground-state population through M-photon ionization.

In particular, we expect that, in our case where $M=2$, the third-harmonic generation will be enhanced near the photon absorption minimum. First we plot $\chi^{(3)}$ as given in (9) in Fig. 4(a), which shows that at low intensities a detuning ϵ close to zero is the optimum detuning for harmonic generation. In fact, $|\chi^{(3)}|^2$ attains its maximum at the detuning (for q_{c2c1} large)

$$\epsilon=\frac{q+q_{c2c1}}{(q+q_{c2c1})^2+q^2q_{c2c1}^2-1}. \tag{11}$$

For higher intensities, however, the dynamics (ionization in

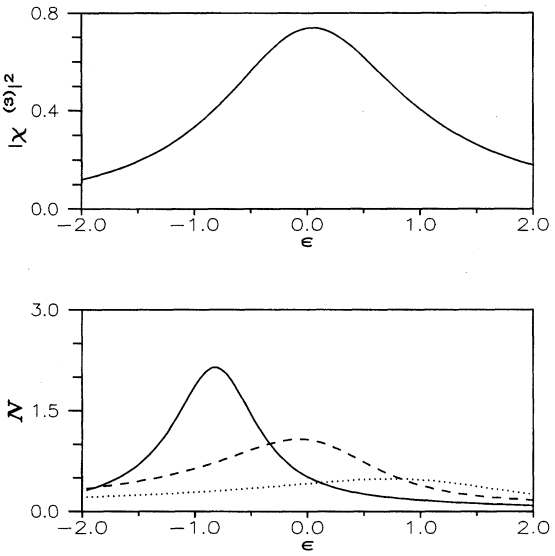

FIG. 4. Upper graph: $|\chi^{(3)}|^2$ as a function of the detuning. Lower graph: Third-harmonic generation as a function of detuning. The solid curve corresponds to a laser intensity $I=3.16\times10^{10}$ W/cm^2, the dashed curve to $I=1.0\times10^{11}$ W/cm^2, and the dotted curve to $I=1.41\times10^{11}$ W/cm^2.

particular) becomes important. In order to investigate this, we calculate numerically the third-order nonlinear polarizability by

$$P^{(3)}(t)=\int \mu_{gc2}U^*_{c2}(t)U_g(t)dE_{c2}. \tag{12}$$

The number of third-harmonic photons generated at each instance of time is then proportional to $|P^{(3)}(t)|^2$. Examples of the third-harmonic generation for different laser intensities are shown in Fig. 4(b). We plot the total harmonic production in the long-time limit, which is proportional to

$$N=\int_0^\infty |P^{(3)}(t)|^2dt, \tag{13}$$

as a function of the detuning ϵ. The optimum detuning for harmonic generation is now indeed found to be close to the absorption minimum (10), and is in fact always shifted towards the detuning (11), irrespective of the sign of q and q_{c2c1}. The profile for the harmonic generation is asymmetric, reflecting the presence of the AI resonance (see also [2]).

It is interesting to observe that the harmonic generation is not always an increasing function of the intensity. There are two reasons for this: First, without any incoherent decay, when $\bar\gamma_g=0$, the harmonic generation tends to be maximum at detuning $\epsilon=0$. Thus, the optimum intensity is that at which the photon absorption minimum (10) is at zero detuning, in our case at $I=10^{11}$ W/cm^2. Second, the presence of incoherent decay ($\bar\gamma_g=0.1\gamma_g$ in our case), which increases with increasing intensity, favors even smaller intensities, so that the optimum intensity is lower than $I=10^{11}$ W/cm^2, as is clear from Fig. 4(b).

Let us finally note that all these effects are essentially due to destructive interferences between the two different paths leading to continuum $|c_1\rangle$, one direct path, the other through the AI resonance. The presence of other, noninterfering paths determines ultimately how deep the minimum in ionization can be, and how efficient the harmonic generation consequently is. In the system treated here, the incoherent decay channels are represented by $\bar\gamma_g$. If this decay exceeds the "coherent" decay to $|c_1\rangle$, the interferences will be washed out. The only requirement to observe the effects described above is $\bar\gamma_g<\gamma_g$.

IV. CONCLUSIONS

We analyzed the excess photon ionization through an AI resonance, where we included a perturbative but exact treatment of the C-C coupling. We showed that both excess photon ionization and harmonic generation can be enhanced, not only because of the presence of the intermediate resonance, but mainly due to a minimum in photon absorption. In general, we showed analytically that the quantum interferences that lead to the absorption minimum near an M-photon resonant AI state, maximize the $(M+1)$-photon coupling. As a consequence, the $(M+1)$st-order nonlinear process is enhanced, without having the depletion due to M-photon ionization.

We applied the theory to, and performed explicit calculations on, a two-photon resonant AI system. We derived photoelectron spectra, ionization profiles, and studied the third-harmonic generation, both perturbatively (calculating the third-order susceptibility $\chi^{(3)}$) and by including the full dynamics of the system. The intensity dependence of the harmonic generation is strongly nonperturbative as a result of interference effects. Around the photon detuning given in (10), the harmonic generation is optimized due to the simultaneous occurrence of the suppression of two-photon ionization and the enhancement of the three-photon coupling.

ACKNOWLEDGMENTS

The work of S.J.v.E. was supported by the Human Capital and Mobility program under Contract No. ERBCHBICT941512.

APPENDIX

Here we give a derivation of the relevant equations describing the atomic system displayed in Fig. 1, using the resolvent operator. For further details we refer to [13].

Starting from the full Hamiltonian for atoms and fields one first eliminates the nonresonant bound and continuum states. One is thus left with an effective Hamiltonian H describing the evolution of the resonant states $|g\rangle$, $|\tilde c1\rangle$, and $|c2\rangle$, which includes the field-dependent decay width $\bar\gamma_g$ of the ground state to other continua than $|\tilde c1\rangle$ and $|c2\rangle$, an effective M-photon dipole operator $D^{(M)}$ coupling the ground state to $|\tilde c1\rangle$, and a one-photon dipole operator D coupling $|\tilde c1\rangle$ and $|c2\rangle$.

The equations for the various matrix elements of the resolvent operator $G(z)=1/(z-H)$ read then

$$(z-\tilde{E}_g)G_{gg}-\int D^{(M)}_{g\tilde{c}1}G_{\tilde{c}1g}d\tilde{E}_{\tilde{c}1}=1, \tag{A1a}$$

$$(z-\tilde{E}_{\tilde{c}1})G_{\tilde{c}1g}-D^{(M)}_{\tilde{c}1g}G_{gg}-\int D_{\tilde{c}1c2}G_{c2g}d\tilde{E}_{c2}=0, \tag{A1b}$$

$$(z-\tilde{E}_{c2})G_{c2g}-\int D_{c2\tilde{c}1}G_{\tilde{c}1g}d\tilde{E}_{\tilde{c}1}=0. \tag{A1c}$$

Here the ground-state energy is $\tilde{E}_g=E_g-i\bar{\gamma}_g$ and the continuum energies $\tilde{E}_{\tilde{c}1}=E_{\tilde{c}1}-M\hbar\omega$ and $\tilde{E}_{c2}=E_{c2}-(M+1)\hbar\omega$ already take into account the photon energies.[1]

The M-photon dipole coupling energy $D^{(M)}_{g\tilde{c}1}$ can be specified as the product of the M-photon dipole moment, defined in Sec. II A and the Mth power of the (slowly varying) electric field amplitude, $\mu^{(M)}_{g\tilde{c}1}\mathscr{E}(t)^M$, and similarly the one-photon dipole coupling is $D_{\tilde{c}1c2}=\mu_{\tilde{c}1c2}\mathscr{E}(t)$. The time dependence of $\mathscr{E}$ will henceforth be suppressed.

The C-C coupling between $|\tilde{c}1\rangle$ and $|c2\rangle$ cannot be treated exactly, unless by making some simplifying assumptions. Instead we treat this coupling perturbatively, which is valid for sufficiently low intensity. In the lowest-order perturbation limit, neglecting the coupling to $|c2\rangle$ in the equations for G_{gg} and $G_{\tilde{c}1g}$ for the moment, we get

$$G_{gg}(z)=\frac{1}{z-\tilde{E}_g-\int[|D^{(M)}_{g\tilde{c}1}|^2/(z-\tilde{E}_{\tilde{c}1})]d\tilde{E}_{\tilde{c}1}}. \tag{A2}$$

The integral in the denominator of Eq. (A2) can be calculated explicitly, provided $\mu^{(M)}_{gc1}$ can be approximated as constant near the poles of the integral, which is correct for the coupling to a pure continuum without resonances (see Sec. II A). Defining the dimensionless quantity $x=(z-E_a+M\hbar\omega)/\gamma_a$ we have

$$\begin{aligned}\int\frac{|D^{(M)}_{g\tilde{c}1}|^2}{z-\tilde{E}_{\tilde{c}1}}d\tilde{E}_{\tilde{c}1}&=\frac{\gamma_g}{\pi}\int_{-\infty}^{\infty}\frac{(\epsilon_{c1}+q)^2}{(x-\epsilon_{c1})(1+\epsilon_{c1}^2)}d\epsilon_{c1}\\&=-\gamma_g\left(i-\frac{(q-i)^2}{(x+i)}\right)\\&=-\gamma_g\left[i\frac{(q+x)^2}{x^2+1}+\frac{2q+(1-q^2)x}{x^2+1}\right],\end{aligned} \tag{A3}$$

where $\gamma_g=\pi|\mu^{(M)}_{gc1}|^2\mathscr{E}^{2M}$ is the decay rate to the pure continuum $|c1\rangle$. This integral determines the effective energy shift and decay rate of the ground state due to the coupling to $|\tilde{c}_1\rangle$. With the definition for the normalized photon detuning $\epsilon=(E_g+M\hbar\omega-E_a)/\gamma_a$, we get

$$\begin{aligned}G_{gg}(x)&=\frac{1}{\gamma_a(x-\epsilon)+\gamma_g[i-(q-i)^2/(x+i)]+i\bar{\gamma}_g}\\&\equiv\frac{x+i}{\gamma_a(x-x_+)(x-x_-)},\end{aligned} \tag{A4}$$

where the roots $x_\pm$ satisfy

$$x^2+\left(i-\epsilon+i\frac{\gamma_g+\bar{\gamma}_g}{\gamma_a}\right)x-\frac{\gamma_g}{\gamma_a}(q^2-2iq)-i\epsilon-\frac{\bar{\gamma}_g}{\gamma_a}=0. \tag{A5}$$

It then follows from Eq. (A1) that

$$G_{\tilde{c}1g}(x)=\frac{\mu^{(M)}_{\tilde{c}1g}\mathscr{E}^M(x+i)}{\gamma_a^2(x-\epsilon_{c1})(x-x_+)(x-x_-)}. \tag{A6}$$

This result reduces for $\bar{\gamma}_g=0$ to previous results calculated by other authors [13,17]. Substituting Eq. (A6) into Eq. (A1), we derive

$$G_{c2g}(x)=\frac{\pi\mu_{c2c1}\mu^{(M)}_{c1g}\mathscr{E}^{M+1}}{\gamma_a^2}\frac{qq_{c2c1}-i(x+q+q_{c2c1})}{(x-\epsilon_{c2})(x-x_+)(x-x_-)}, \tag{A7}$$

where $\epsilon_{c2}\equiv(E_{c2}-\hbar\omega-E_a)/\gamma_a$. Higher-order corrections can be obtained by substituting this result for G_{c2g} in the equations for G_{c1g} and G_{gg}, solving them, and substituting the result in (A1c), etc. We will not give the resulting complicated expressions, but note that we included these corrections in the numerical calculations of Sec. III.

Now we are ready to calculate the time-dependent amplitude of each state, using the transformation

$$U_\alpha(t)=\frac{i\gamma_a}{2\pi}\lim_{\eta\to0}\int_{-\infty}^{\infty}e^{-ix\gamma_a t}G_{\alpha g}(x+i\eta)dx, \tag{A8}$$

for $\alpha=g,\tilde{c}1,c2$, from which the photoelectron and ionization spectra can directly be derived. The results were given in Sec. II B.

[1]Here we implicitly make the rotating wave approximation. With respect to the C-C coupling this is correct if there is no resonant coupling from $|\tilde{c}1\rangle$ to $|c2\rangle$ by photon *emission*. Here we assume that, indeed, $M-1$ photons are not sufficient to reach the threshold of the second continuum $|c2\rangle$.

[1] U. Fano, Phys. Rev. **124**, 1866 (1961).
[2] L. Armstrong and B. L. Beers, Phys. Rev. Lett. **34**, 1290 (1975).
[3] G. Alber and P. Zoller, Phys. Rev. A **27**, 1373 (1983), and references therein.
[4] S. J. van Enk, Jian Zhang, and P. Lambropoulos, Phys. Rev. A **50**, 3362 (1994); Appl. Phys. B **60**, S141 (1995).
[5] T. F. Gallagher, R. Kachru, N. H. Tran, and H. B. van Linden van den Heuvell, Phys. Rev. Lett. **51**, 1753 (1983).
[6] H. Stapelfeldt and H. K. Haugen, Phys. Rev. Lett. **69**, 2638 (1992).
[7] H. Stapelfeldt, P. Kristensen, U. Ljungblad, and T. Anderson, Phys. Rev. A **50**, 1618 (1994).
[8] A. T. Georges, P. Lambropoulos, and J. H. Marburger, Phys. Rev. A **15**, 300 (1977).
[9] B. Walker *et al.*, Phys. Rev. A **48**, R894 (1993).
[10] N. J. van Druten, R. Trainham, and H. G. Muller, Phys. Rev. A **50**, 1593 (1994).
[11] D. Charalambidis *et al.*, Phys. Rev. A **50**, R2822 (1994).
[12] M. V. Fedorov and A. E. Kazakov, Prog. Quantum Electron. **13**, 1 (1989).
[13] P. Lambropolous and P. Zoller, Phys. Rev. A **24**, 379 (1981).
[14] Y. S. Kim and P. Lambropoulos, Phys. Rev. A **29**, 3159 (1984).
[15] X. Tang, Z. Phys. **6**, 255 (1987).
[16] K. Rzążewski and R. Grobe, Phys. Rev. Lett. **54**, 1729 (1985).
[17] K. Rzążewski and J. H. Eberly, Phys. Rev. Lett. **47**, 408 (1981).
[18] This has been estimated from structure calculations in He.
[19] P. E. Coleman and P. L. Knight, J. Phys. B **15**, L235 (1982).